

# Magnetic field effect for two electrons in a two-dimensional random potential

Giuliano Benenti<sup>1,2,3</sup> and Dima L. Shepelyansky<sup>1</sup>

<sup>1</sup>Laboratoire de Physique Quantique, UMR 5626 du CNRS, Université Paul Sabatier, 31062 Toulouse Cedex 4, France

<sup>2</sup>International Center for the Study of Dynamical Systems, Università degli Studi dell'Insubria, via Valleggio 11, 22100 Como, Italy

<sup>3</sup>Istituto Nazionale di Fisica della Materia, Unità di Milano, via Celoria 16, 20133 Milano, Italy

(Received 28 November 2000; published 10 May 2001)

We study the problem of two particles with Coulomb repulsion in a two-dimensional disordered potential in the presence of a magnetic field. For the regime when without interaction all states are well localized, it is shown that above a critical excitation energy electron pairs become delocalized by interaction. The transition between the localized and delocalized regimes is similar to the metal-insulator transition at the mobility edge in the three-dimensional Anderson model with broken time reversal symmetry.

DOI: 10.1103/PhysRevB.63.235103

PACS number(s): 71.30.+h, 72.15.Rn, 05.45.Mt

## I. INTRODUCTION

The interplay of disorder and interactions in electronic systems is a central problem in condensed matter physics.<sup>1</sup> Two-dimensional (2D) systems are of particular interest, since the scaling theory of localization<sup>2</sup> predicts that noninteracting electrons are always localized in a 2D disordered potential, while a metal-insulator transition has been reported in transport measurements with 2D electron and hole gases.<sup>3</sup> The study of this many-body problem is very complicated, for both analytical and numerical analysis. It is therefore highly desirable to have some relatively simple models that could be solved and would lead to a better understanding of the effects of interactions in the presence of disorder. The problem of two interacting particles (TIP's) in a random potential has received much attention in the last few years. It has been shown<sup>4</sup> that TIP's can propagate coherently for a length  $l_c$  that is much larger than the one-particle localization length  $l_1$ , which can lead to an enhancement of transport.<sup>5</sup> This problem has been studied recently by different groups in one<sup>4-11</sup> and two dimensions<sup>12-15</sup> and it has been understood that the pair delocalization is related to the enhancement of interaction in systems with complex, chaotic eigenstates. The delocalization factor is determined by the density of two-particle states coupled by the interaction,  $\rho_2$ , and by the interaction induced transition rate  $\Gamma_e$ . At  $\kappa_e = \Gamma_e \rho_2 \sim 1$  the interaction matrix elements become comparable with the two-particle level spacing and the collisions between particles give a strong increase of the ratio  $l_c/l_1$ .

Most studies of the TIP problem have considered a short range interaction. In this case, when two particles are localized at a distance  $R \gg l_1$ , the overlap of their wave functions is exponentially small, and such states are localized in much the same way as in the noninteracting case. On the other hand, when the average distance between particles is larger than  $l_1$ , the screening of charges in the case with a given charge density is problematic. Because of that for such a regime it is natural to consider the bare Coulomb interaction in the simple TIP problem. Recently, it has been shown<sup>15</sup> that the Coulomb repulsion can delocalize two particles (electrons) in a two-dimensional disordered lattice, even if the particles are separated by a distance  $R \gg l_1$ . The delocalization of two-electron states takes place in a way similar to

the single-particle Anderson transition in three dimensions. Indeed, the pair center of mass moves in the 2D plane, while electrons rotate around it, which gives an effective third dimension. The rotation occurs on a ring of width  $l_1$  and radius  $R \propto l_1^{4/3}$  fixed by energy conservation. As a result the two-particle states are delocalized for excitation energies  $\epsilon > \epsilon_c \propto l_1^{-4/3}$  ( $\kappa_e > 1$ ).<sup>15</sup> This expectation has been confirmed numerically<sup>15</sup> by a study of the level spacing statistics  $P(s)$ , which displays a transition from the Poisson distribution (for  $\epsilon < \epsilon_c$ ) to the Wigner-Dyson distribution (for  $\epsilon > \epsilon_c$ ). It was also found that at a critical point ( $\epsilon = \epsilon_c$ ) the  $P(s)$  statistics is close to the distribution found in the 3D Anderson model at the mobility edge.<sup>16,17</sup>

In this paper we consider the effect of a magnetic field on the TIP problem with Coulomb repulsion in two dimensions. We summarize our findings as follows: (1) we numerically compute TIP wave functions and give direct evidence that the Coulomb interaction leads to delocalization of excited states; (2) we show that with increase of the excitation energy the level spacing statistics  $P(s)$  exhibits a transition from the Poisson distribution to the Wigner-Dyson distribution and that at the critical point  $P(s)$  is similar to the critical statistics found in the 3D Anderson model with broken time reversal symmetry.<sup>18</sup>

The paper is organized as follows. The model is introduced in Sec. II. In Sec. III we review the analytical arguments developed<sup>15</sup> for the TIP problem in two dimensions with Coulomb repulsion and we discuss the influence of a magnetic field on this theory. In Secs. IV and V we discuss our numerical data for this problem when the time reversal symmetry is broken by a magnetic field. A number of typical examples of interaction induced pair delocalization is shown in Sec. IV. The transition in the level spacing statistics from the Poisson distribution to the Wigner-Dyson distribution is analyzed in Sec. V. There we present a comparison of our results with the data for the 3D Anderson transition with time reversal symmetry broken by a magnetic field. In Sec. VI we present a summary of the results.

## II. THE MODEL

We consider two particles with Coulomb repulsion in a two-dimensional disordered square lattice, in the presence of

a constant magnetic field perpendicular to the plane. We restrict our investigations to the triplet case, which corresponds to the study of two spinless fermions. The singlet case, investigated in one and two dimensions for the on-site Hubbard interaction,<sup>12</sup> should give similar results. The Hamiltonian of the model reads

$$H = - \sum_{\langle \mathbf{r}, \mathbf{r}' \rangle} V_{\mathbf{r}, \mathbf{r}'} c_{\mathbf{r}}^\dagger c_{\mathbf{r}'} + \sum_{\mathbf{r}} E_{\mathbf{r}} n_{\mathbf{r}} + H_{int}. \quad (1)$$

The vectors  $\mathbf{r} = (x, y)$  denote the  $L \times L$  sites of a square lattice with periodic boundary conditions applied in both directions;  $c_{\mathbf{r}}^\dagger$  ( $c_{\mathbf{r}}$ ) creates (destroys) an electron at the site  $\mathbf{r}$ . The occupation number at the site  $\mathbf{r}$  is  $n_{\mathbf{r}} = c_{\mathbf{r}}^\dagger c_{\mathbf{r}}$ . The uncorrelated random energies  $E_{\mathbf{r}}$  are distributed with constant probability within the interval  $[-W/2, W/2]$ , where  $W$  denotes the magnitude of the disorder. The nearest neighbor hopping terms on the square lattice include the magnetic field, and are given by  $V_{\mathbf{r}, \mathbf{r}'} = V \exp(\pm i 2\pi \alpha y)$  for  $\mathbf{r} - \mathbf{r}' = (\pm 1, 0)$ , while for  $\mathbf{r} - \mathbf{r}' = (0, \pm 1)$  they are  $V_{\mathbf{r}, \mathbf{r}'} = V$ . This choice corresponds to the Landau gauge for the vector potential  $\mathbf{A} = (-Bya, 0, 0)$ , with the magnetic field  $B$  perpendicular to the plane. The number of flux quanta per unit cell of the lattice is  $\alpha = eBa^2/h = Ba^2/\phi_0$  and in the following the lattice spacing constant  $a$  is taken to be unity. The magnetic field is chosen to be commensurate with the lattice, i.e.,  $\alpha = k/L$ , with  $k$  integer. The last term in Eq. (1) gives the interaction:

$$H_{int} = \frac{U}{2} \sum_{\mathbf{r} \neq \mathbf{r}'} \frac{n_{\mathbf{r}} n_{\mathbf{r}'}}{|\mathbf{r} - \mathbf{r}'|}, \quad (2)$$

where  $U$  is the strength of the Coulomb repulsion and  $|\mathbf{r} - \mathbf{r}'|$  is the interparticle nearest distance computed on a 2D torus.

### III. ANALYTICAL ESTIMATES

We consider the case with the average distance between electrons  $R = |\mathbf{r}_1 - \mathbf{r}_2|$  much larger than their one-particle localization length:  $R \gg l_1$ . In the localized regime the one-body Anderson localized orbitals can be represented in the lattice basis as

$$\phi_{\alpha}(\mathbf{r}) \approx \frac{1}{l_1} \exp\left(-\frac{|\mathbf{r} - \bar{\mathbf{r}}_{\alpha}|}{l_1} + i\theta_{\alpha}(\mathbf{r})\right), \quad (3)$$

where  $\bar{\mathbf{r}}_{\alpha}$  marks the center of the localized  $\alpha$ th single-particle eigenstate, and  $\theta_{\alpha}(\mathbf{r})$  is a random phase. Interaction matrix elements between noninteracting two-particle eigenstates  $|\alpha\beta\rangle$  and  $|\gamma\delta\rangle$  are given by

$$\langle \gamma\delta | H_{int} | \alpha\beta \rangle = Q_{\alpha\beta}^{\gamma\delta} - Q_{\alpha\beta}^{\delta\gamma}, \quad (4)$$

with

$$Q_{\alpha\beta}^{\gamma\delta} = U \sum_{\mathbf{r} \neq \mathbf{r}'} \frac{\phi_{\alpha}(\mathbf{r}) \phi_{\beta}(\mathbf{r}') \phi_{\gamma}^*(\mathbf{r}) \phi_{\delta}^*(\mathbf{r}')}{|\mathbf{r} - \mathbf{r}'|}. \quad (5)$$

Due to one-particle exponential localization, Coulomb repulsion can induce electron jumps only inside the localiza-

tion domain of size  $l_1$ . Therefore, when  $R \gg l_1$ , it is possible to expand the interaction for electron displacements  $\Delta\mathbf{r}_1, \Delta\mathbf{r}_2$  of typical length  $l_1$  near their initial positions  $\mathbf{r}_1, \mathbf{r}_2$ . The terms up to the first order in the expansion of the Coulomb potential give only mean-field corrections to the one-particle potential. The first term beyond mean field has a dipole-dipole form, and is of the order of

$$U_{dd} \sim -\frac{U}{R^3} \Delta\mathbf{r}_1 \cdot \Delta\mathbf{r}_2 \sim \frac{U l_1^2}{R^3}. \quad (6)$$

This gives dipole-dipole matrix elements between noninteracting eigenstates:

$$(Q_{\alpha\beta}^{\gamma\delta})_{dd} \sim -\frac{U}{R^3} \sum_{\mathbf{r}_1, \mathbf{r}_2} \Delta\mathbf{r}_1 \cdot \Delta\mathbf{r}_2 \phi_{\alpha}(\mathbf{r}_1) \phi_{\beta}(\mathbf{r}_2) \phi_{\gamma}^*(\mathbf{r}_1) \phi_{\delta}^*(\mathbf{r}_2). \quad (7)$$

The sum in Eq. (7) runs over  $l_1^2$  sites for each electron, so that in total the sum contains of the order of  $l_1^4$  terms with random signs. Each term is of the order of  $l_1^2 \phi^4 \sim l_1^{-2}$ . As a result, the typical dipole-dipole transition matrix element in the ergodic approximation and with eigenstates given by Eq. (3) is of the order of

$$Q_{dd}^{\text{typ}} \approx \frac{U}{R^3}. \quad (8)$$

On the basis of this result we can estimate the typical interaction induced transition rate  $\Gamma_e$  between noninteracting two-particle eigenstates by means of the Fermi golden rule:

$$\Gamma_e \sim (Q_{dd}^{\text{typ}})^2 \rho_2 \sim \frac{U^2 l_1^4}{R^6 V}. \quad (9)$$

Here we took the density of states coupled by the interaction in the middle of the energy band of width  $B \sim V$ , i.e.,  $\rho_2 \sim l_1^4/V$ . Due to localization, one-electron jumps over a distance larger than  $l_1$  give exponentially small matrix elements and these transitions can be excluded from consideration. The mixing of two-electron states takes place when

$$\kappa_e = \Gamma_e \rho_2 \sim \left(\frac{U l_1^4}{V R^3}\right)^2 > 1, \quad (10)$$

which corresponds to  $R < l_1 (U l_1 / V)^{1/3}$ . For  $U \sim V$  one gets  $R < l_1^{4/3}$ , and the condition  $R \gg l_1$  is still satisfied when  $l_1 \gg 1$ .<sup>19</sup> Therefore the physical picture is qualitatively different from the case of a short range screened interaction, where mixing is possible only for states at a distance  $R < l_1$ . For  $\kappa_e > 1$  the pair jumps on a typical length  $l_1$  and its diffusion rate is

$$D_e \sim l_1^2 \Gamma_e \sim \frac{V \kappa_e}{l_1^2}. \quad (11)$$

The transition from localization to pair diffusion takes place in a way qualitatively similar to that in the Anderson

model in 3D. The pair center of mass can move in the 2D plane and in addition the electrons diffusively rotate around it in a ring of radius  $R$  and width  $l_1$ , keeping their Coulomb energy  $E_{ee} \sim U/R$  constant. The number of effective sites in the third direction,  $M_{ef} \approx \pi R/l_1$ , is given by the number of circles of size  $l_1$  in the ring. Therefore, following standard results for the quasi-2D Anderson model,<sup>20</sup> the pair localization length  $l_c$  is given by

$$\frac{l_c}{l_1} \sim \exp(M_{ef}g_2) \sim \exp\left(\frac{\pi R \kappa_e}{l_1}\right), \quad (12)$$

where  $g_2 \sim \kappa_e$  is the two-particle conductance<sup>5</sup> and the above estimate is valid in the metallic phase for the corresponding 3D Anderson model ( $\kappa_e > 1$ ). Since  $R \sim l_1^{4/3}$  when  $\kappa_e \sim 1$  (for  $U \sim V$ ), at the transition the TIP localization length jumps from  $l_c \sim l_1$  to an exponentially large value

$$l_c \sim l_1 \exp(\pi l_1^{1/3}). \quad (13)$$

The TIP diffusion will eventually be localized due to the finite number of planes in the third direction. However, if disorder is not too strong ( $l_1 \gg 1$ ), the Coulomb interaction gives rise to an exponentially sharp localization length enhancement, with a ‘‘critical’’ behavior similar to that the 3D Anderson model for finite system sizes  $l_c \gg L \gg l_1$ . We remark that, due to disorder, the ring is not rigid and the electronic motion adapts to the fluctuations of the random potential so that the total energy remains constant even with some variation of the ring radius. This effect should increase the number of planes  $M_{ef}$  of the effective quasi-2D Anderson model, giving a stronger delocalization effect.

Since the excitation energy  $\epsilon$  is related to the pair distance,  $\epsilon \sim U/R$ , the condition of pair delocalization ( $k_e > 1$ ) implies

$$\epsilon > \epsilon_c \propto l_1^{-4/3}; \quad (14)$$

the scaling relation  $\epsilon_c l_1^{4/3} = \text{const}$  is in agreement with the numerical results obtained in Ref. 15.

Finally we discuss the influence of a magnetic field on the theory presented in this section. For a typical magnetic field corresponding to  $\alpha = 1/6$  flux quanta per plaquette, the disorder strengths  $W = 7V$  and  $W = 10V$  are strong enough to mix different Landau levels, as illustrated in Fig. 1 (top): the single-particle density of states at  $W = 7V$  is only slightly changed with respect to the zero magnetic field case. In Fig. 1 (bottom) we evaluate the energy dependence of the single-particle inverse participation ratio  $\xi_1$  (IPR):

$$\xi_1 = 1/\sum_{\mathbf{r}} |\phi(\mathbf{r})|^4, \quad l_1 \sim \sqrt{\xi_1}. \quad (15)$$

This convenient characteristic  $\xi_1$  determines how many sites contribute to an eigenstate and is simply related to the localization length  $l_1$ . The magnetic field gives an increase of  $\xi_1$  in the middle of the energy band. It is known from weak localization<sup>20</sup> that, in the presence of a magnetic field, coherent time-reversed paths are eliminated and therefore back-scattering is suppressed. On the contrary, the magnetic field shrinks the band and at  $W = 7V$  there is a slight reduction of

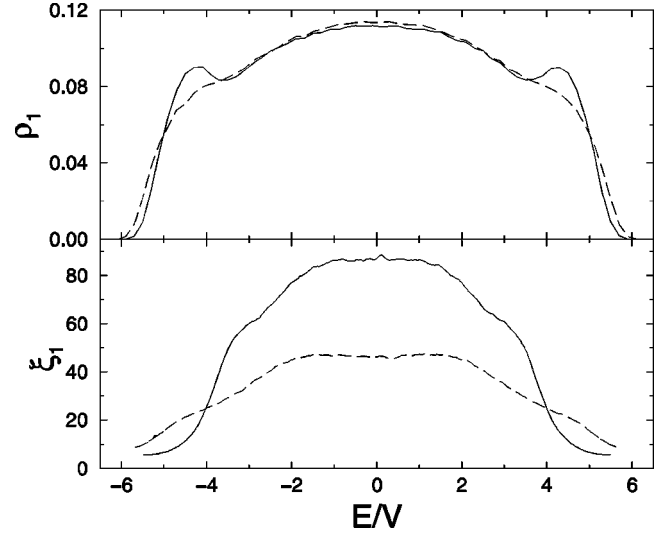


FIG. 1. Single-particle density of states  $\rho_1$  (top) and inverse participation ratio  $\xi_1 \sim l_1^{-2}$  (bottom) in the 2D Anderson model as a function of energy, for system size  $L = 24$ , disorder strength  $W = 7V$ , and rescaled magnetic field  $\alpha = 1/6$  (full line) and  $\alpha = 0$  (dashed line). Data are averaged over  $N_R = 10^3$  disorder realizations.

the density of states near the band edges, which brings about a decrease in  $l_1$ .<sup>21</sup> For the parameters of Fig. 1 the results found in Ref. 15 give the critical delocalization energy  $\epsilon_c \approx 1.2V$ , counted from the energy of the ground state [Fig. 1(c) there], which corresponds to  $E \approx -3.8V$  in Fig. 1 here. At this energy  $\xi_1(\alpha = 1/6) \approx \xi_1(\alpha = 0)$  [see Fig. 1 (bottom)] which implies  $l_1(\alpha = 1/6) \approx l_1(\alpha = 0)$ , and hence we expect that the critical energy for the delocalization transition in the presence of a magnetic field will remain approximately the same:  $\epsilon_c(\alpha = 1/6) \approx \epsilon_c(\alpha = 0)$ .<sup>22</sup>

#### IV. TIP DELOCALIZATION

In order to study the eigenstate properties of our model with interaction, we diagonalize the Hamiltonian (1) numerically. In this way we determine the two-particle probability distribution  $F_k(\mathbf{r}_1, \mathbf{r}_2) = |\Psi_k(\mathbf{r}_1, \mathbf{r}_2)|^2$  for the  $k$ th eigenfunction  $\Psi_k(\mathbf{r}_1, \mathbf{r}_2) = \langle \mathbf{r}_1 \mathbf{r}_2 | \Psi_k \rangle$  written in the lattice basis. From this we extract the one-particle probability,

$$f_k(\mathbf{r}_1) = \sum_{\mathbf{r}_2} F_k(\mathbf{r}_1, \mathbf{r}_2), \quad (16)$$

and the probability of the interparticle distance,

$$f_{dk}(\mathbf{R}) = \sum_{\mathbf{r}_2} F_k(\mathbf{R} + \mathbf{r}_2, \mathbf{r}_2) \quad (17)$$

with  $\mathbf{R} = \mathbf{r}_1 - \mathbf{r}_2$ .

Typical examples of probability distributions are shown in Fig. 2 at  $W = 10V$  for a system size  $L = 30$ . They clearly show that the two-particle ground state [Fig. 2 (top)] remains localized in the presence of interaction, with the particles staying far from each other in order to minimize Coulomb repulsion. Similar conclusions apply to low-energy eigen-

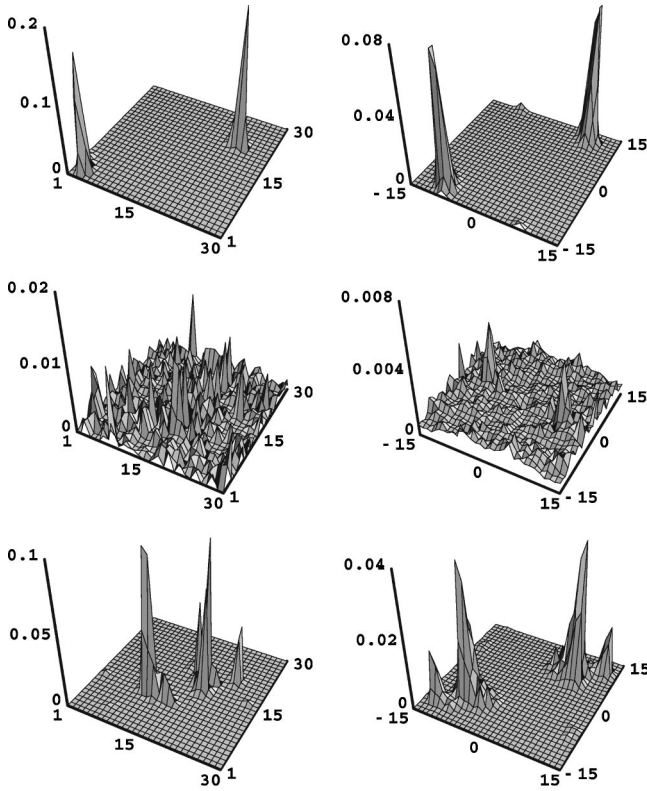


FIG. 2. Probability distributions  $f$  (left) and  $f_d$  (right) from Eqs. (16) and (17) for two interacting particles in a 2D lattice of size  $L=30$ , with disorder strength  $W=10V$ , and rescaled magnetic field  $\alpha=1/6$ . Top: Coulomb repulsion  $U=2V$ , ground state, number of sites occupied by one particle given by IPR  $\xi_s=8$ ; middle:  $U=2V$ , rescaled one-electron excitation energy  $\epsilon/B=0.71$  ( $B=4V$ ),  $\xi_s=320$ ; bottom: same excitation energy but at  $U=0$ ,  $\xi_s=14.7$ .

states. On the contrary, for higher excitation energies [ $\epsilon/B=0.71$  in Fig. 2 (middle), where  $\epsilon=\delta E/2$ , the excitation energy of the TIP eigenstate  $\delta E$  is counted from the ground state, and  $B=4V$  is the bandwidth at  $W=0$ ] the probability distribution  $f$  spreads over the whole lattice, while  $f_d$  shows a hole at small  $R$  and a depletion for large  $R$ . The first property is a simple consequence of Coulomb repulsion, while the second one is in agreement with the general discussion of the model (1). Following the analytical arguments<sup>15</sup> summarized in Sec. III, we believe that this ring structure [see also Fig. 3 (top)] would become more evident at larger system sizes, with maximum interparticle distance  $R_{\max} \approx L/2 \gg l_1^{4/3}$ .<sup>23</sup> It is impossible to fully satisfy such a condition within numerically tractable system sizes, if one considers that the condition  $l_1 \gg 1$  should be satisfied at the same time.<sup>24</sup> We stress that this pair delocalization takes place in a regime of strong localization for the one-particle wave functions. This is demonstrated in Fig. 2 (bottom) and Fig. 3 (bottom), which show the probability distributions for the noninteracting problem ( $U=0$ ) at the same excitation energy. As a quantitative measure of the interaction induced charge delocalization one can take the inverse participation ratio  $\xi_s$  for the one-particle probability  $f$ :

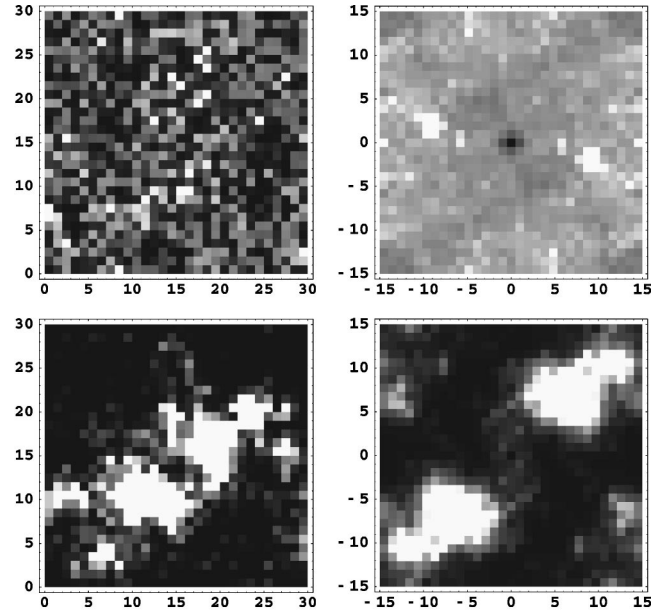


FIG. 3. Density plots for the case of Fig. 2 (middle) (two top plots,  $U=2V$ ) and for the case of Fig. 2 (bottom) (two bottom plots,  $U=0$ ). Black corresponds to the minimum of the probability distribution and white to the maximum (color plots are available at <http://arXiv.org/abs/cond-mat/0011461>).

$$\xi_s = 1 / \sum_{\mathbf{r}_1} f^2(\mathbf{r}_1). \quad (18)$$

In this way  $\xi_s$  gives the number of lattice sites occupied by one particle in an eigenstate. For the case of Fig. 2, the Coulomb interaction does not significantly change  $\xi_s \approx 8$  for the ground state, while for an excitation energy  $\epsilon/B=0.71$  there is a huge delocalization effect from  $\xi_s=14.7$  at  $U=0$  to  $\xi_s=320$  at  $U=2V$ .

## V. SPECTRAL STATISTICS

The qualitative change of the structure of the eigenstates also leads to a change in the level spacing statistics. In the one-particle problem spectral fluctuations proved to be a very useful tool to characterize the 3D Anderson transition.<sup>25</sup> Localized wave functions yield uncorrelated spectra with Poisson statistics, characterized by a distribution  $P(s)$  of the energy spacings between successive levels going to

$$P_P(s) = \exp(-s) \quad (19)$$

when the system size  $L \gg l_1$ . Delocalized wave functions yield correlated spectra and Wigner-Dyson statistics with the Wigner surmise

$$P_U(s) = \frac{32s^2}{\pi^2} \exp\left(-\frac{4s^2}{\pi}\right) \quad (20)$$

in the absence of time reversal symmetry. The striking advantage of such an approach is that it deals only with the spectrum and does not involve heavy numerical calculations of conductivity or eigenfunctions.

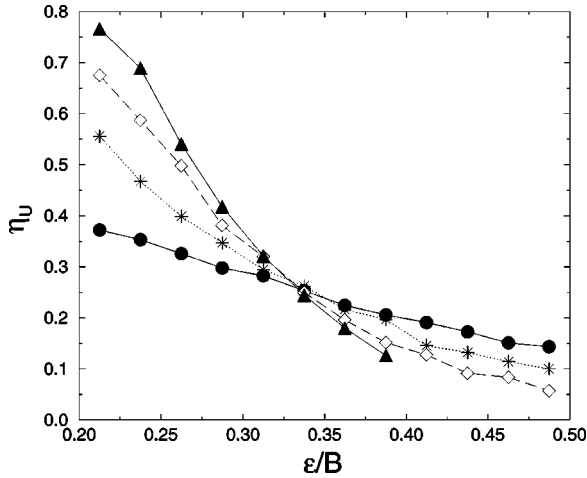


FIG. 4. Dependence of  $\eta_U$  on the rescaled one-electron energy  $\epsilon/B$  for  $W=7V$ ,  $\alpha=1/6$ ,  $U=2V$ , system sizes  $L=6$  (circles, number of disorder realizations  $N_R=2\times 10^4$ , number of spacings for each point of the graph  $N_S>4\times 10^4$ ),  $L=12$  (stars,  $N_R=5\times 10^2$ ,  $N_S>1.1\times 10^4$ ),  $L=18$  (diamonds,  $N_R=10^2$ ,  $N_S>1.4\times 10^4$ ), and  $L=24$  (triangles,  $N_R=10$ ,  $N_S>3\times 10^3$ ).

To analyze the evolution of the  $P(s)$  distribution with respect to the excitation energy, it is convenient to use the parameter

$$\eta_U = \frac{\int_0^{s_U} [P(s) - P_U(s)] ds}{\int_0^{s_U} [P_P(s) - P_U(s)] ds}, \quad (21)$$

where  $s_U=0.5076\dots$  is the first intersection point of  $P_P(s)$  and  $P_U(s)$ . In this way  $P_P(s)$  corresponds to  $\eta_U=1$  and  $P_U(s)$  to  $\eta_U=0$ . The dependence of  $\eta_U$  on the one-electron excitation energy  $\epsilon=\delta E/2$  is shown in Fig. 4. This figure shows that, at fixed interaction  $U=2V$ , disorder  $W=7V$ , and rescaled magnetic field  $\alpha=1/6$ , curves at different system sizes  $6\leq L\leq 24$  intersect at  $\epsilon_c/B\approx 0.33$ , with  $\eta_{Uc}\approx 0.26$ . While for  $\epsilon<\epsilon_c$  the level spacing statistics approaches the Poisson limit ( $\eta_U\rightarrow 1$ ) when the system size increases, for  $\epsilon>\epsilon_c$  the tendency is toward the Wigner-Dyson distribution ( $\eta_U\rightarrow 0$ ). We note that the critical excitation energies at  $W=7V$  and  $W=10V$  ( $\epsilon_c\approx 0.67$ , data not shown) are similar to the values found in, Ref. 15 in agreement with the expectations of Sec. III.

The level spacing statistics  $P(s)$  is shown in Fig. 5 near the ground state and for excitation energies  $\epsilon>\epsilon_c$ , for a system size  $L=18$ . The transition from Poisson to Wigner-Dyson statistics is evident.

The  $P(s)$  statistics near the critical point  $\epsilon=\epsilon_c$  is shown in Fig. 6. The curves at different system sizes display a size-independent intermediate distribution, which exhibits level repulsion  $P(s)\propto s^2$  at small  $s$  and a Poisson-like tail  $P(s)\propto \exp(-as)$ , with  $a\approx 1.9$ . The close agreement between these distributions and the critical statistics found in the 3D Anderson model with broken time reversal symmetry at the mobility edge, taken from Ref. 18, supports the analytical argu-

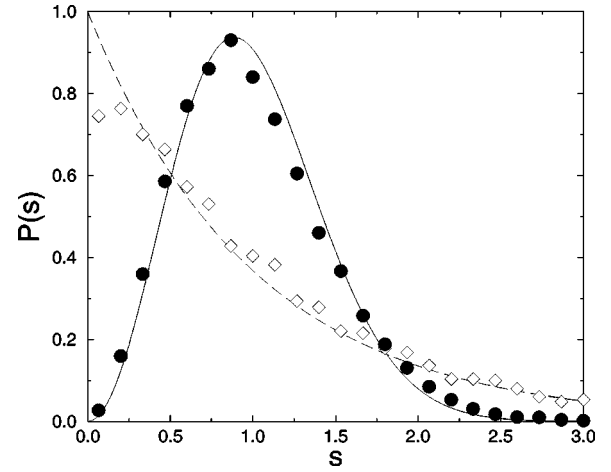


FIG. 5. Transition from the Poisson distribution (dashed curve) to the Wigner surmise (full curve) in the level statistics  $P(s)$  for the case of Fig. 4 at  $L=18$ :  $0<\epsilon/B<0.1$  (diamonds,  $\eta_U=0.89$ ,  $N_S=4.5\times 10^3$ ) and  $0.47<\epsilon/B<0.5$  (circles,  $\eta_U=0.06$ ,  $N_S=3.5\times 10^4$ ).

ments given in Sec. III. This 3D critical statistics also gives a good approximation for the 2D critical statistics at  $W=10V$  (see Fig. 6), with  $\eta_{Uc}\approx 0.29$ . The small difference in the  $\eta_{Uc}$  values at  $W=7V$ , and  $10V$  (already observed at  $\alpha=0$ ; see Ref. 15) can be attributed to the fact that the jump in the localization length at the ‘‘transition,’’  $l_c/l_1\sim \exp(\pi l_1^{1/3})$ , is not sufficiently sharp. This is due to the not very large values of  $l_1$  accessible for numerical simulations. Investigation of cases with larger  $l_1$  would require a significant increase of the system size, in order to satisfy the condition  $L>R\approx l_1^{4/3}$ . We also note that the finite statistics and the limited system sizes prevent us from precisely evaluating the critical excitation energy  $\epsilon_c$  and the critical value  $\eta_{Uc}$ .

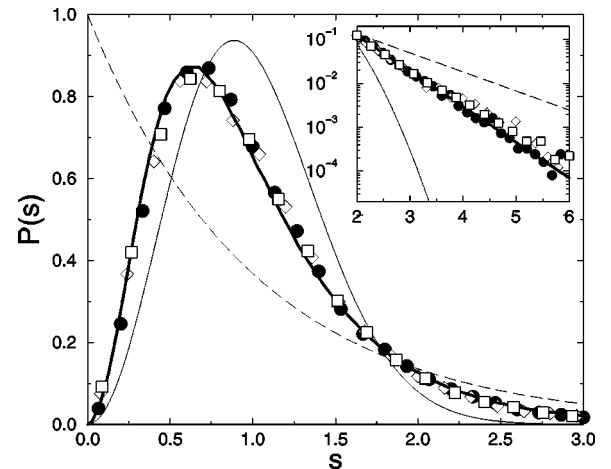


FIG. 6. Level statistics  $P(s)$  at the critical point, for  $U=2V$  and  $\alpha=1/6$ :  $W=7V$ ,  $0.32<\epsilon/B<0.35$ ,  $L=6$  (circles,  $N_S=8\times 10^4$ ) and  $L=18$  (diamonds,  $N_S=2\times 10^4$ );  $W=10V$ ,  $0.65<\epsilon/B<0.70$ ,  $L=12$  (squares,  $N_R=2\times 10^4$ ,  $N_S=10^5$ ). The thick line shows the critical  $P(s)$  in the 3D Anderson model in the presence of a magnetic field (data taken from Fig. 1 of Ref. 16), with the large- $s$  exponential decay  $P(s)\propto \exp(-\kappa s)$ ,  $\kappa=1.87$ , shown in the inset.

## VI. CONCLUSIONS

We have shown that Coulomb interaction can delocalize electron pairs in a 2D disordered potential in the presence of a magnetic field, above a critical excitation energy, in a way similar to the Anderson transition in 3D. The close relation between these two transitions is reflected in the close similarity of level statistics at the critical point. The results obtained in this paper should be relevant for experiments at

small electron density and/or large disorder fluctuations, when the distance between electrons is larger than the size of their localization length in the absence of interaction.

## ACKNOWLEDGMENTS

We thank Isa Zharekeshev for the possibility of using the data of Ref. 18, and the IDRIS in Orsay and the CICT in Toulouse for access to their supercomputers.

- 
- <sup>1</sup>*Disorder and Interaction in Transport Phenomena*, edited by M. Schreiber, special issue of *Ann. Phys. (Leipzig)* **8**, 539 (1999).
- <sup>2</sup>E. Abrahams, P.W. Anderson, D.C. Licciardello, and T.V. Ramakrishnan, *Phys. Rev. Lett.* **42**, 673 (1979).
- <sup>3</sup>E. Abrahams, S.V. Kravchenko, and M.P. Sarachik, *Rev. Mod. Phys.* **73**, 251 (2000).
- <sup>4</sup>D.L. Shepelyansky, *Phys. Rev. Lett.* **73**, 2607 (1994).
- <sup>5</sup>Y. Imry, *Europhys. Lett.* **30**, 405 (1995).
- <sup>6</sup>D. Weinmann, A. Müller-Groeling, J.-L. Pichard, and K. Frahm, *Phys. Rev. Lett.* **75**, 1598 (1995).
- <sup>7</sup>F. von Oppen, T. Wettig, and J. Müller, *Phys. Rev. Lett.* **76**, 491 (1996).
- <sup>8</sup>I.V. Ponomarev and P.G. Silvestrov, *Phys. Rev. B* **56**, 3742 (1997).
- <sup>9</sup>P.H. Song and D. Kim, *Phys. Rev. B* **56**, 12 217 (1997).
- <sup>10</sup>M. Leadbeater, R.A. Römer, and M. Schreiber, *Eur. Phys. J. B* **8**, 643 (1999).
- <sup>11</sup>*Correlated Fermions and Transport in Mesoscopic Systems*, edited by T. Martin, G. Montambaux, and J. Trân Thanh Vân (Editions Frontières, Gif-sur-Yvette, 1996).
- <sup>12</sup>M. Ortuño and E. Cuevas, *Europhys. Lett.* **46**, 224 (1999); E. Cuevas, *Phys. Rev. Lett.* **83**, 140 (1999).
- <sup>13</sup>R.A. Römer, M. Leadbeater, and M. Schreiber, *Ann. Phys. (Leipzig)* **8**, 675 (1999).
- <sup>14</sup>J. Talamantes and M. Pollak, *Phys. Rev. B* **62**, 12 785 (2000).
- <sup>15</sup>D.L. Shepelyansky, *Phys. Rev. B* **61**, 4588 (2000); see also *Quantum Physics at Mesoscopic Scale*, edited by C. Glattli, M. Sanquer, and J. Trân Thanh Vân (EDP Sciences, Les Ulis, 2000), p. 99.
- <sup>16</sup>I.Kh. Zharekeshev and B. Kramer, *Phys. Rev. Lett.* **79**, 717 (1997).
- <sup>17</sup>D. Braun, G. Montambaux, and M. Pascaud, *Phys. Rev. Lett.* **81**, 1062 (1998).
- <sup>18</sup>M. Batsch, L. Schweitzer, I.Kh. Zharekeshev, and B. Kramer, *Phys. Rev. Lett.* **77**, 1552 (1996).
- <sup>19</sup>For  $U \gg V$  the theory should be modified; see X. Waintal, D. Weinmann, and J.-L. Pichard, *Eur. Phys. J. B* **7**, 451 (1999); F. Selva and J.-L. Pichard, cond-mat/0003338, *Eur. Phys. J. B* (to be published).
- <sup>20</sup>P.A. Lee and T.V. Ramakrishnan, *Rev. Mod. Phys.* **57**, 287 (1985).
- <sup>21</sup>This is consistent with results from the 3D Anderson model in the presence of a magnetic field: at the band center, zero-field localized states near the mobility edge become delocalized, while close to the tail of the band the magnetic field causes localization of extended states; see T. Dröse, M. Batsch, I.Zh. Zharekeshev, and B. Kramer, *Phys. Rev. B* **57**, 37 (1998).
- <sup>22</sup>A more detailed theory should take into account the variation of the transition rate  $\Gamma_e$  and of the density of directly coupled states  $\rho_2$  with the excitation energy  $\epsilon$ .
- <sup>23</sup>A ring structure in  $f_d$  has been observed in the TIP problem with long-range attractive interaction by J. Lages and D.L. Shepelyansky, cond-mat/0002296, *Eur. Phys. J. B* (to be published). This interaction can be considered as an effective harmonic attraction coming from the expansion of the Coulomb repulsion near  $R \sim U/\epsilon$ .
- <sup>24</sup>We note that  $L=30$  corresponds to a large Hilbert space dimension  $N_H \approx 4 \times 10^5$  and that numerical diagonalization of such matrices is possible thanks to the Lanczos algorithm, with special care to find eigenvalues in the interior of the spectrum; see J. Cullum and R.A. Willoughby, *J. Comput. Phys.* **44**, 329 (1981).
- <sup>25</sup>B.I. Shklovskii, B. Shapiro, B.R. Sears, P. Lambrianides, and H.B. Shore, *Phys. Rev. B* **47**, 11 487 (1993).